AD-A238 034 EFFECT OF CLADDING THICKNESS ON ATTENUATION IN UNIFORMLY CURVED SINGLE-MODE OPTICAL FIBERS(U) NAVAL WEAPONS CENTER CHINA LAKE CA P L OVERFELT ET AL 1/1

UNCLASSIFIED SEP 90 NWC-TP-7104 XN-NAVAIR NL

END
FILMED
DTIC

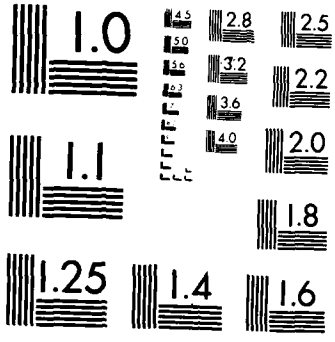

NWC TP 7104

Effect of Cladding Thickness on Attenuation in Uniformly Curved Single-Mode Optical Fibers

by
P. L. Overfelt
Research Department
and
G. A. Hewer
Intercept Weapons Department

SEPTEMBER 1990

NAVAL WEAPONS CENTER
CHINA LAKE, CA 93555-6001

Naval Weapons Center

FOREWORD

The work described in this report was performed at the Naval Weapons Center during fiscal year 1990 for the SKYRAY Fiber Optics Data Link Project under NAVAIR Task A932932I/008C/63737. SKYRAY is funded by the DOD Balanced Technology Initiative and is managed by Naval Air Systems Command 921, Rick Habayeb.

This work was reviewed for technical accuracy by Charles S. Kenney.

Approved by
R. L. DERR, *Head*
Research Department
29 August 1990

Under authority of
D. W. COOK
Capt., USN
Commander

Released for publication by
W. B. PORTER
Technical Director

NWC Technical Publication 7104

Published by . . . . . Technical Information Department
Collation . . . . . Cover, 13 leaves
First printing . . . . . 55 copies

REPORT DOCUMENTATION PAGE

Form Approved
OMB No. 0704-0188

1. AGENCY USE ONLY (*Leave blank*)	2. REPORT DATE	3. REPORT TYPE AND DATES COVERED
	1990, September	Final, 90 Jan to 90 Aug

4. TITLE AND SUBTITLE

EFFECT OF CLADDING THICKNESS ON ATTENUATION IN UNIFORMLY CURVED SINGLE-MODE OPTICAL FIBERS

5. FUNDING NUMBERS

NAVAIR Task
A932932I/008C/63737

6. AUTHOR(S)

Overfelt, P. L., and Hewer, G. A.

7. PERFORMING ORGANIZATION NAME(S) AND ADDRESS(ES)

Naval Weapons Center
China Lake, CA 93555-6001

8. PERFORMING ORGANIZATION REPORT NUMBER

NWC TP 7104

9. SPONSORING/MONITORING AGENCY NAME(S) AND ADDRESS(ES)

Naval Air Systems Command
Dr. Rick Habayeb, Code 921
Arlington, VA 22202

10. SPONSORING/MONITORING AGENCY REPORT NUMBER

11. SUPPLEMENTARY NOTES

12a. DISTRIBUTION/AVAILABILITY STATEMENT

Approved for public release; distribution is unlimited.

12b. DISTRIBUTION CODE

13. ABSTRACT (*Maximum 200 words*)

This report analyzes the effect of finite cladding thickness on attenuation loss in uniformly curved single-mode optical fibers. An approximate electromagnetic analysis valid for relatively small cladding thicknesses and fiber radii of curvature in the centimeter to millimeter range is presented. Numerical results for fibers used in actual SKYRAY Fiber Optics Project field tests are presented and discussed.

14. SUBJECT TERMS

Optical Fibers, Attenuation, Uniform Curvature, Finite Cladding Thickness

15. NUMBER OF PAGES

23

16. PRICE CODE

17. SECURITY CLASSIFICATION OF REPORT	18. SECURITY CLASSIFICATION OF THIS PAGE	19. SECURITY CLASSIFICATION OF ABSTRACT	20. LIMITATION OF ABSTRACT
UNCLASSIFIED	UNCLASSIFIED	UNCLASSIFIED	UL

1. INTRODUCTION

Electromagnetic analyses of attenuation in uniformly curved singly clad optical fibers usually do not account for the finite cladding radius of the fiber (References 1 through 3). For many standard fibers, the cladding-to-core-radius ratio is quite large (at least 20); thus, most analysis techniques assume that the cladding radius is infinite. When this "infinite" cladding radius assumption is not used, it is necessary to consider very simplified analyses for attenuation loss resulting from curvature in optical waveguides with double or multiple claddings (References 4 and 5). These methods are approximate and are based on (1) the weak guidance assumption, (2) continuation of wave functions (Reference 6), and (3) change of the axial phase constant, as the result of uniform bending. They are applicable to both small and large radii of curvature.

Since we are interested in applying any analysis of attenuation resulting from curvature of an optical fiber to the SKYRAY Fiber Optics Project, we have verified that the above assumptions are acceptable for dealing with a high-speed fiber payout scenario. It has been shown that at high speeds the "peel point" radius of curvature may be only a few millimeters. Thus, one of the primary considerations for any analysis method is its ability to compute attenuation losses for relatively small bend radii. The method of Section 2 will handle such small bends.

For the numerical analysis of determining the effect of cladding thickness on attenuation resulting from curvature, we have used the optical parameters of four fibers that were payed out in previous SKYRAY field tests. These fibers are

(1) AT&T dispersion-shifted fiber (DSF)
(2) AT&T tethered vehicle fiber (TVF)
(3) Corning payout fiber
(4) Corning SMF/DS (single-mode fiber/dispersion-shifted)

At the present time, all of the above fibers have a standard cladding diameter of ~125 μm. Assuming mode field diameters on the order of 5 to 8 μm, this implies that the cladding-to-core-radius ratio is around 15 to 20. Future options are tending to lower the cladding diameter to ~80 μm (and sometimes less), resulting in cladding-to-core-radius ratios of 9 or 10. We must be able to assess whether and how attenuation resulting from uniform curvature will be affected by such small ratios.

Section 2 provides a description of the analysis method for uniformly curved optical fibers with finite claddings. Section 3 uses the results of Section 2 to plot cladding thickness versus attenuation with the normalized radius of curvature as a parameter. Section 4 contains our conclusions and recommendations.

2. ATTENUATION IN A CURVED SINGLE-MODE OPTICAL FIBER WITH A FINITE CLADDING THICKNESS

The geometry of a curved fiber with circular cross section and finite cladding thickness is shown in Figure 1. The fiber is assumed to have a constant radius of curvature R, core radius a, and cladding radius b. n_1, n_2, and n_3 are the indices of refraction in the core, cladding, and outer sections of the fiber, respectively. Throughout the following, we will refer to the cladding-to-core-radius ratio as b/a. The actual cladding thickness d is given by

$$d = b - a \quad , \tag{1}$$

and the normalized cladding thickness is

$$\frac{d}{a} = \frac{b}{a} - 1 \quad . \tag{2}$$

Following Reference 5, we obtain a simplified power attenuation coefficient given by

$$2\alpha(R) = \frac{4b\kappa^2}{\beta V^2 K_1^2(\gamma a)} \int_0^{\phi_0} \frac{\bar{\sigma}(b)\,\bar{\gamma}^2(b)}{u[\bar{\gamma}^2(b) + \bar{\sigma}^2(b)]} \exp[-2u]d\phi \quad . \tag{3}$$

We can define the variables in Equation 3 as follows:

$$\kappa^2 = n_1^2 k_o^2 - \beta^2 \quad , \tag{4a}$$

$$\gamma^2 = \beta^2 - n_2^2 k_o^2 \quad , \tag{4b}$$

$$\sigma^2 = \begin{cases} n_3^2 k_o^2 - \beta^2 \; ; \; n_3 > n_2 \\ \beta^2 - n_3^2 k_o^2 \; ; \; n_3 < n_2 \end{cases} \quad , \tag{4c}$$

where κ, γ, and σ are the transverse propagation constants in the core, cladding, and outer regions, respectively.

By assuming that a curved fiber can be described as an equivalent straight fiber with an inhomogeneous refractive index distribution, we obtain

$$\bar{\gamma}^2(b) = \beta^2 - n_2^2\left(1 + \frac{2b\cos\phi}{R}\right)k_o^2 \quad , \tag{5a}$$

$$\bar{\sigma}^2(b) = \begin{cases} n_3^2\left(1 + \frac{2b\cos\phi}{R}\right)k_o^2 - \beta^2 \; ; \; n_3 > n_2 \\ \beta^2 - n_3^2\left(1 + \frac{2b\cos\phi}{R}\right)k_o^2 \; ; \; n_3 < n_2 \end{cases} \quad , \tag{5b}$$

$$u = \begin{cases} \frac{R[\gamma^3 - \bar{\gamma}^3(b)]}{3k_o^2 n_2^2 \cos\phi} \; ; \; \phi \neq \frac{\pi}{2} \\ \gamma b \qquad\qquad ; \; \phi = \frac{\pi}{2} \end{cases} \quad , \tag{5c}$$

$$V^2 = k_o{}^2 a^2 \, (n_1{}^2 - n_2{}^2) \quad , \tag{6a}$$

$$k_o = \frac{2\pi}{\lambda_o} \quad . \tag{6b}$$

λ_o is the free-space wavelength, typically in the 1.3- to 1.6-μm range, K_1 is a modified Hankel function of order 1, and β is the axial propagation constant.

Equation 3 must be integrated numerically over the local angle ϕ (see Figure 1). Note that the upper limit of this integration is not explicitly defined. This is because the value of ϕ_o is dependent upon the values of ϕ and R in certain cases. For large enough values of the bending radius R, ϕ_o has the value π. However, as R decreases, the averaged transverse propagation constant $\bar{\sigma}(b)$ approaches zero. We can define a critical radius for $\phi = 0$ where $\bar{\sigma}(b)$ is zero as

$$R_{c_1} = \frac{2bn_3^2k_o^2}{\sigma^2} \quad . \tag{7}$$

If $\bar{\sigma}(b)$ reaches zero before the integration variable ϕ reaches π, then ϕ_o must be defined as

$$\phi_o = \begin{cases} \cos^{-1}\left[-\dfrac{R}{R_{c_1}}\right] & ; \; n_3 > n_2 \\ \cos^{-1}\left[\dfrac{R}{R_{c_1}}\right] & ; \; n_3 < n_2 \; . \end{cases} \tag{8}$$

This is the point at which radiation is no longer escaping from the fiber. When $\bar{\gamma}(b)$ becomes zero at $\phi = 0$, we have another critical radius, i.e.,

$$R_{c_2} = \frac{2bn_2^2k_o^2}{\gamma^2} \; . \tag{9}$$

At R_{c_2}, we have the usual evanescent field becoming a radiation field while it is still inside the cladding region. When R_{c_2} is reached, we must use the curvature loss formula for singly clad fibers (References 3 and 7). For a single-mode fiber with a single cladding, the cladding radius is assumed to be infinite and we have

$$2\alpha(R) = \frac{\sqrt{\pi}\kappa^2 \exp\left[-\dfrac{2\gamma^3 R}{3\beta^2}\right]}{2V^2\gamma^{3/2}R^{1/2}K_1^2(\gamma a)} \; , \tag{10}$$

which is not a function of b, the cladding radius.

Once integrated, the attenuation coefficient of Equation 3 can be presented either in absolute terms in the practical units dB/Km, or it can be normalized with respect to the attenuation coefficient of a straight fiber. The only restriction on Equation 3 is that the cladding thickness cannot be very small. For small values of the cladding thickness, we must integrate a much more complicated equation consisting of modified Bessel and Hankel functions (References 5 and 8). Also, we should realize that Equation 3 is more accurate as the radius of curvature increases.

3. NUMERICAL RESULTS

As mentioned in the previous section, we have several sets of plots showing the normalized cladding thickness (d/a) versus attenuation with the

normalized radius of curvature (R/a) as a parameter. The attenuation is computed either in the practical units of dB/km, or it is normalized to the attenuation loss in a straight fiber, which is given by (Reference 5)

$$2\alpha(\infty) = \frac{4\pi\sigma\gamma\kappa^2 \exp(-2\gamma b)}{V^2\beta K_1^2(\gamma a)[\gamma^2 + \sigma^2]} \quad . \tag{11}$$

As mentioned in the Introduction, we wish to use the optical parameters of actual fibers involved in high-speed payouts. The first fiber we consider is the AT&T DSF. It has a mode-field diameter [viewed as the single-mode analogue of core diameter in multimode fibers (Reference 7)] of 6.3 ± 0.6 μm at a wavelength of 1.3 μm and 7.0 ± 0.6 μm at a wavelength of 1.55 μm. It is a depressed cladding fiber (see Figure 2) and has a refractive index difference between core and cladding (Δ_1) of 0.5 to 1%, where

$$\Delta_1 = \frac{n_1 - n_2}{n_1} \quad . \tag{12}$$

Since it is a depressed cladding fiber, we have assumed $n_3 > n_2$, with the worst case attenuation at $n_3 = n_1$. Figure 3 is a plot of normalized cladding thickness versus normalized attenuation for R/a = 1.0 x 10^4, 2.0 x 10^4, and 3.0 x 10^4 (i.e., 3.5, 7.0, and 10.5 cm), respectively, at 1.55 μm. Figure 3 shows that at a bending radius of 3.5 cm, the ratio of attenuation at this radius to that of the same straight fiber is around 5; whereas, at a bending radius of 7 cm, the attenuation ratio is less than 1.5. This plot shows also that as the cladding thickness increases, attenuation resulting from curvature alone goes up. At 1.3 μm with a core radius of 3.15 μm and the same values of R/a, we see the same behavior. Figures 3 and 4 show the substantial increase in attenuation loss resulting from curvature. Figures 5 and 6 show the same behavior but now in absolute terms. Comparing Figures 5 and 6, we notice that the attenuation at 1.3 μm with a mode-field radius (core radius) of 3.15 μm is much less than at 1.55 μm with a mode-field radius of 3.5 μm for the same cladding thickness.

Figures 7 through 10 show plots of the AT&T tethered vehicle fiber TVF. It has a mode-field radius of 2.5 μm at the 1.3-μm wavelength and a radius of 3.0 μm at the 1.55-μm wavelength. Using a slightly larger refractive index difference of 0.7% (versus 0.5% for the AT&T DSF), we see there is less variation as a function of cladding thickness for various radius of curvature values as compared to the AT&T DSF.

Figures 11 through 14 show plots of the Corning payout fiber. This fiber has an index difference of around 1% and correspondingly smaller mode-field radii, i.e., 2.75 μm at the 1.3-μm wavelength and 3 μm at the 1.55-μm wavelength. As a result of smaller mode-field diameter coupled with a larger refractive index difference than in the AT&T fibers, we find that lower values of absolute attenuation at smaller bend radii are found with this type of fiber.

In Figure 13, when R/a = 1.5 x 10^3 = 4.12 mm at d/a = 8, we have a computed attenuation of <0.01 dB/Km. However, note that at the 1.55-μm wavelength with a mode-field radius of 3 μm, the attenuation at d/a = 8 is much worse. In Figures 13 and 14, we see an instance of the normal field in the cladding turning into a radiation field for which the "infinite" cladding loss formula in Equation 10 must now be used. Since this formula is not dependent on the finite cladding radius b, it gives a constant attenuation in terms of the cladding thickness once the field begins to radiate.

Figures 15 and 16 show plots of the Corning SMF/DS, which has a Δ_1 of 1% and a mode-field diameter of 8.1 ± 0.65 μm at the 1.55-μm wavelength. This fiber is designed to operate in the 1.55-μm window. Figure 16 shows this fiber at a normalized bend radius of R/a = 1000 (4.05 mm). Even for this very small radius, it has a low attenuation for most cladding thickness values.

Figures 3 through 16 are merely representative of how cladding thickness affects attenuation loss resulting from curvature. Generally, we find that reducing the mode-field diameter and simultaneously increasing the refractive index difference (between n_1 and n_2) will improve the attenuation loss. In terms of absolute attenuation, the normalized cladding thickness may be decreased to as little as 7 or 8 and still give small attenuation at small bend radii (such as occur at the "peel point" in a high-speed payout).

4. CONCLUSIONS

Several general trends can be seen concerning attenuation resulting from curvature and the effects of a finite cladding thickness.

- The cladding must remain thick enough to ensure that attenuation loss remains at acceptable levels throughout the wavelength range of operation.

- Attenuation resulting from curvature increases with wavelength.

- As the index of refraction of the outer region decreases (i.e., $n_3 < n_1$), the attenuation loss decreases.

- Reduction of the core radius (or mode-field radius) coupled with increase in the refractive index difference enables the attenuation to remain at acceptable levels for relatively small cladding thickness, even for radii of curvature in the millimeter range.

REFERENCES

1. R. Baets and P. E. Lagasse. "Loss Calculation and Design of Arbitrary Curved Integrated-Optic Waveguides," *J. Opt. Soc. Am.*, Vol. 73 (1983), pp. 177-87.

2. E.-G. Neumann and H.-D. Rudolph. "Radiation From Bends in Dielectric Rod Transmission Lines," *IEEE MTT*, Vol. MTT-23 (1975), pp. 142-49.

3. D. Marcuse. "Curvature Loss Formula for Optical Fibers," *J. Opt. Soc. Am.*, Vol. 66 (1976), pp. 216-20.

4. S. Kawakami, M. Miyagi, and S. Nishida. "Bending Losses of Dielectric Slab Optical Waveguide With Double or Multiple Claddings: Theory," *Appl. Opt.*, Vol. 14, No. 11 (November 1975), pp. 2588-97.

5. D. Marcuse. "Influence of Curvature on the Losses of Doubly Clad Fibers," *Appl. Opt.*, Vol. 21, No. 23 (December 1982), pp. 4208-13.

6. ------. "Bending Losses of the Asymmetric Slab Waveguide," *Bell. System Tech. J.*, Vol. 50 (October 1971), pp. 2551-63.

7. E.-G. Neumann. *Single-Mode Fibers*, Chap. 5. Berlin, Springer Verlag, 1988.

8. V. Shah. "Curvature Dependence of the Effective Cutoff Wavelength in Single Mode Fibers," *J. Lightwave Tech.*, Vol. LT-5 (January 1987), pp. 35-43.

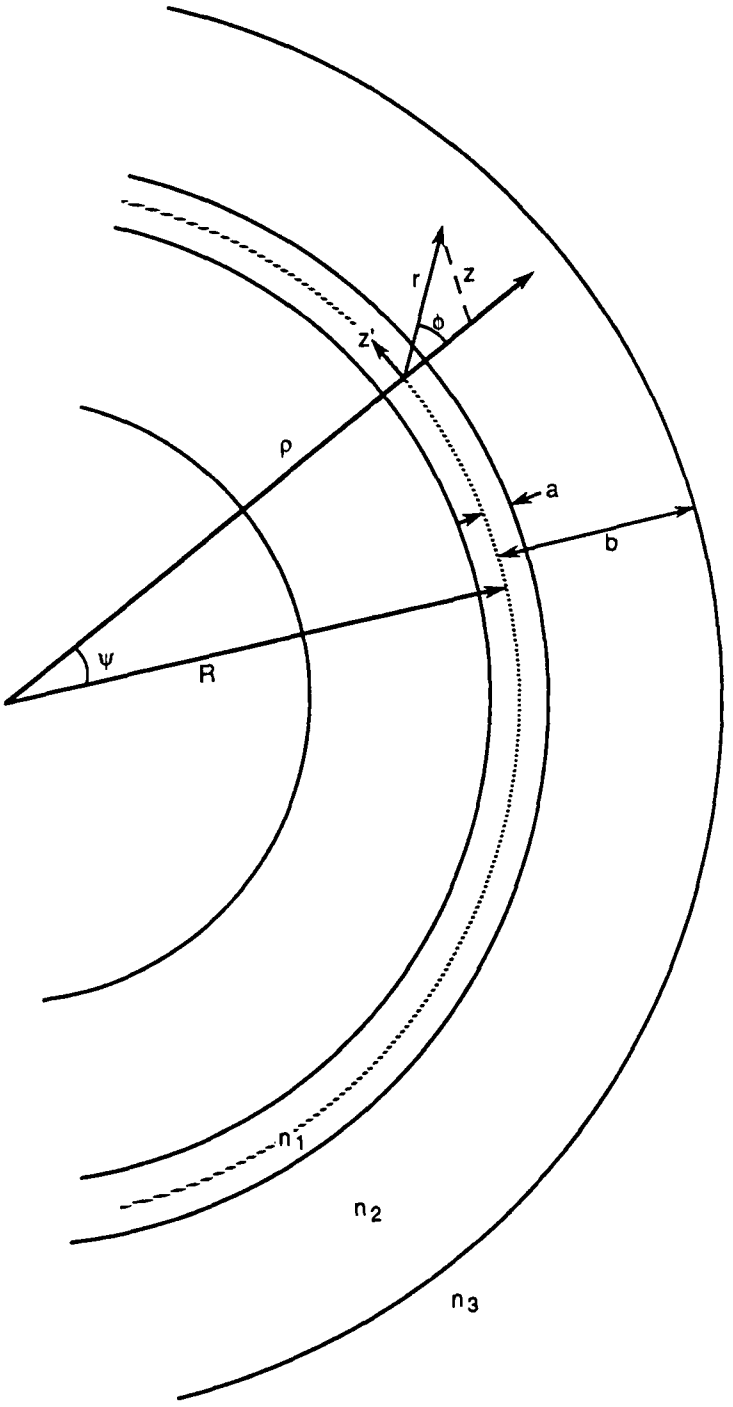

FIGURE 1. Geometry of a Curved Three-Region Optical Fiber.

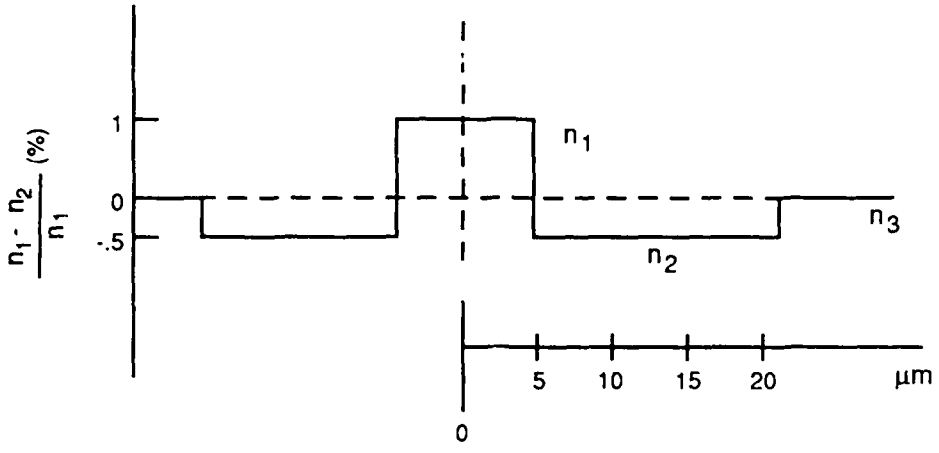

FIGURE 2. Refractive Index Profile of a Typical Depressed Cladding Fiber.

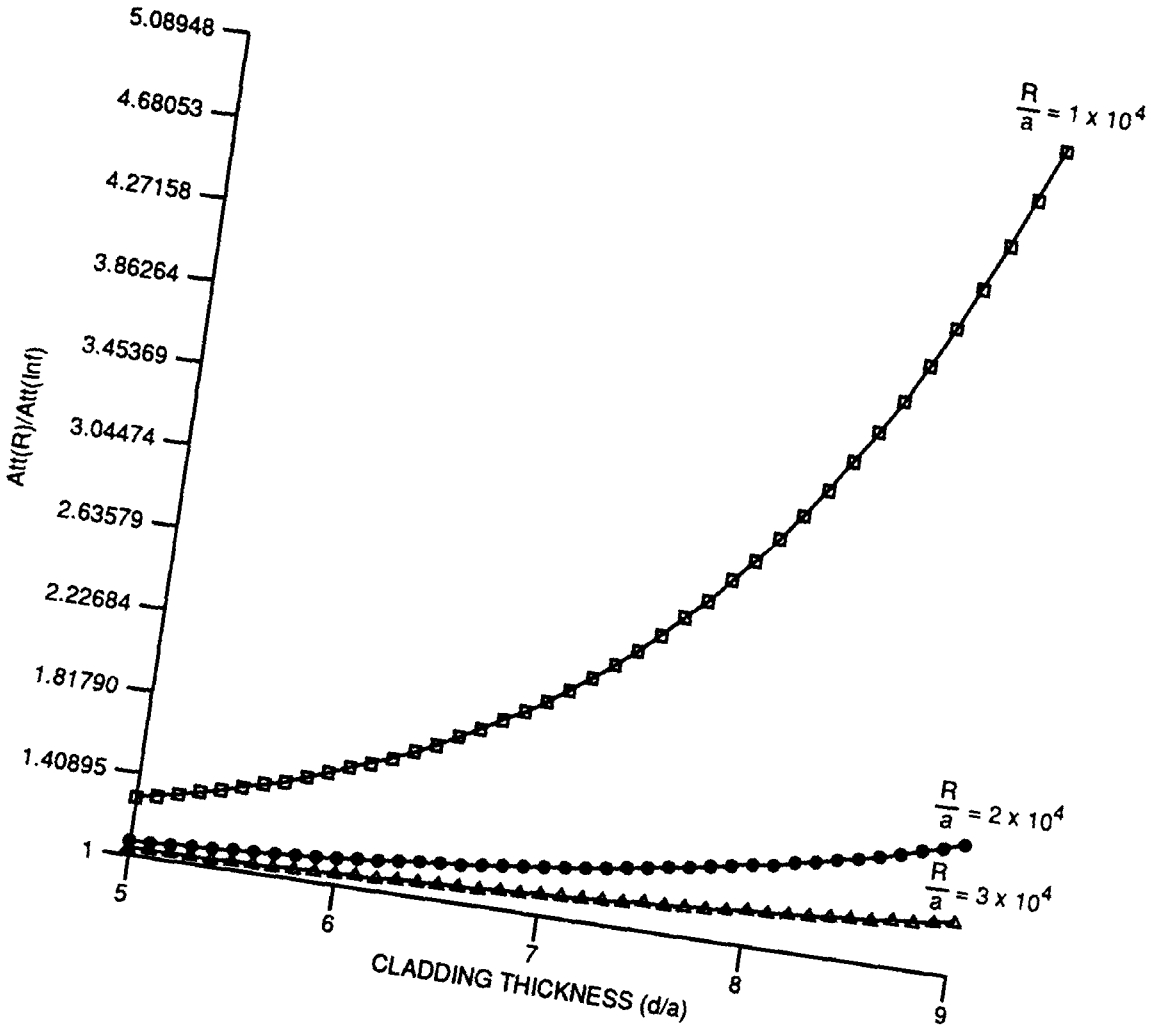

FIGURE 3. Normalized Cladding Thickness Versus Normalized Attenuation for AT&T DSF at 1.55 μm.

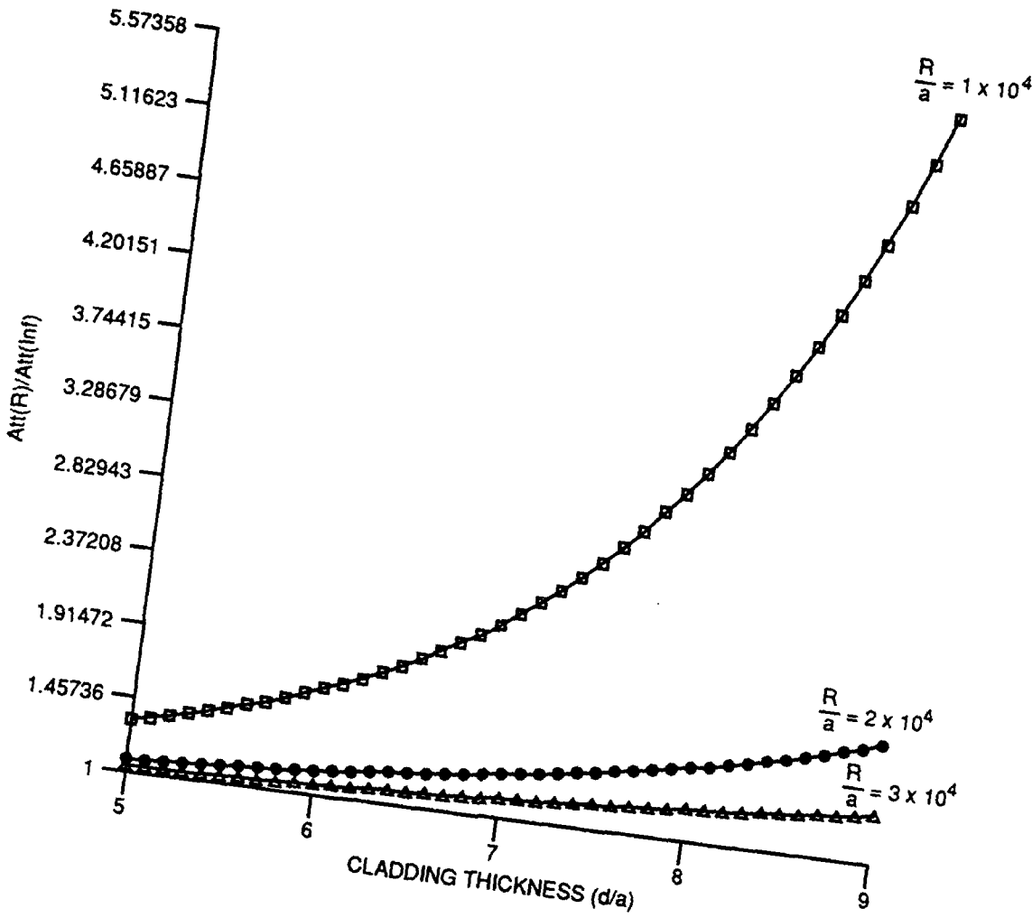

FIGURE 4. Normalized Cladding Thickness Versus Normalized Attenuation for AT&T DSF at 1.3 μm.

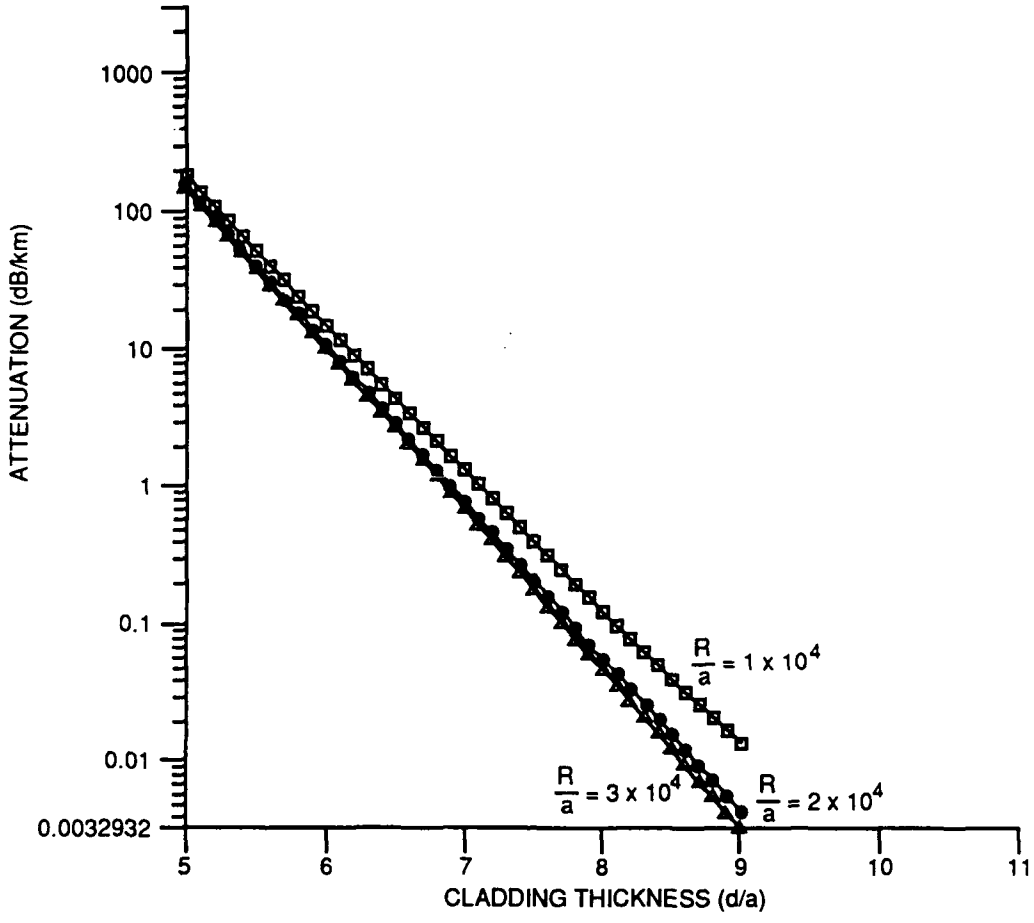

wavelength (μm) = 1.55	n1 = 1.4570
core radius (μm) = 3.50	n2 = 1.4497
Δ_1= .5%	n3 = 1.4570

FIGURE 5. Normalized Cladding Thickness Versus Attenuation for AT&T DSF at 1.55 μm.

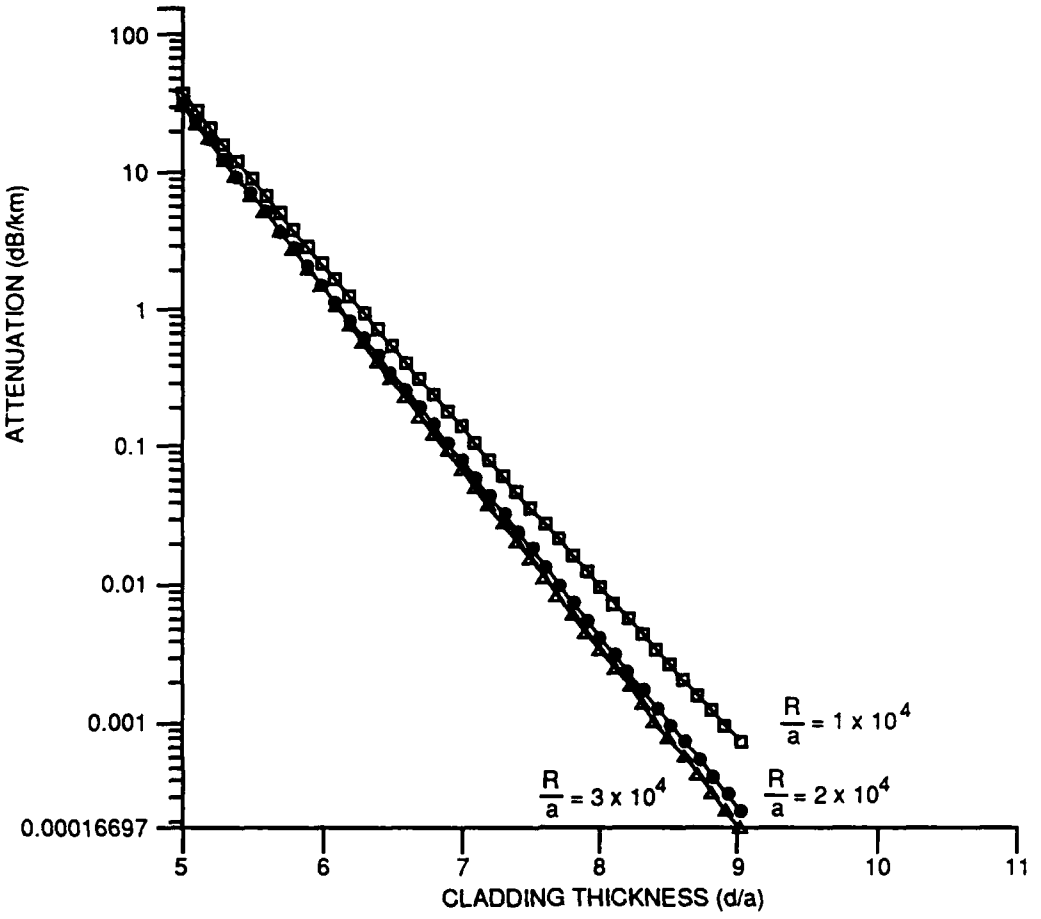

wavelength (μm) = 1.30	n1 = 1.4570
core radius (μm) = 3.15	n2 = 1.4497
Δ_1= .5%	n3 = 1.4570

FIGURE 6. Normalized Cladding Thickness Versus Attenuation for AT&T DSF at 1.3 μm.

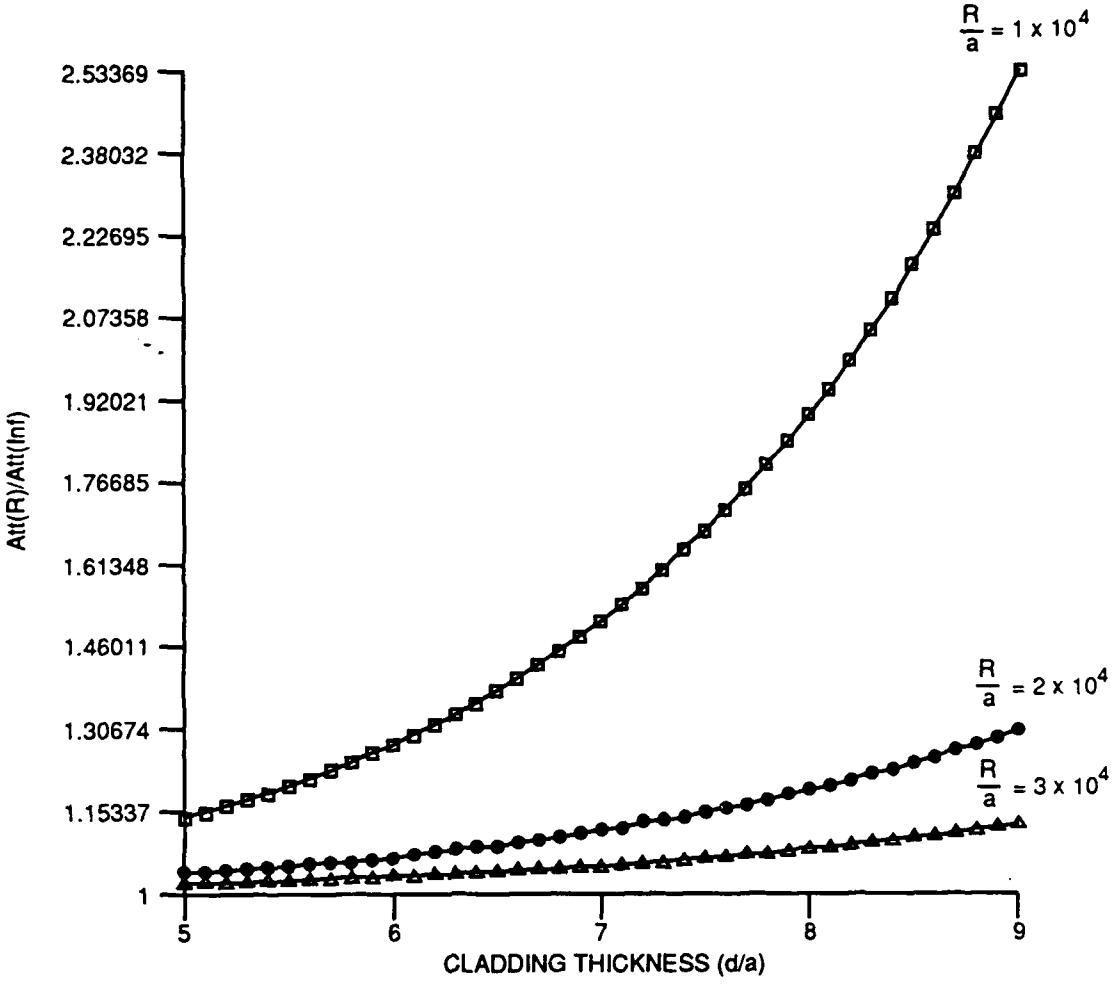

wavelength (μm) = 1.30	n1 = 1.4600
core radius (μm) = 2.50	n2 = 1.4497
Δ_1 = .7%	n3 = 1.4600

FIGURE 7. Normalized Cladding Thickness Versus Normalized Attenuation for AT&T TVF at 1.3 μm.

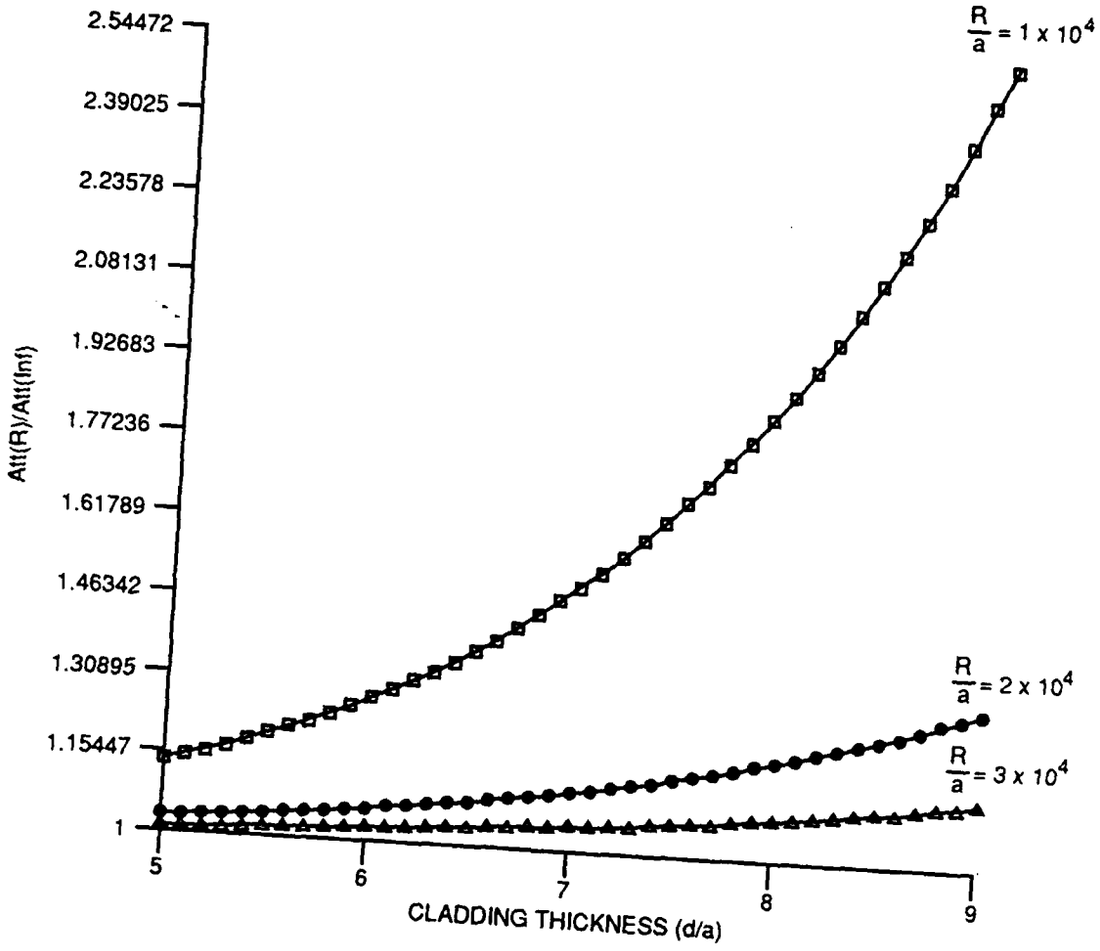

wavelength (μm) = 1.55
core radius (μm) = 3.00
Δ_1= .7%

n1 = 1.4600
n2 = 1.4497
n3 = 1.4600

FIGURE 8. Normalized Cladding Thickness Versus Normalized Attenuation for AT&T TVF at 1.55 μm.

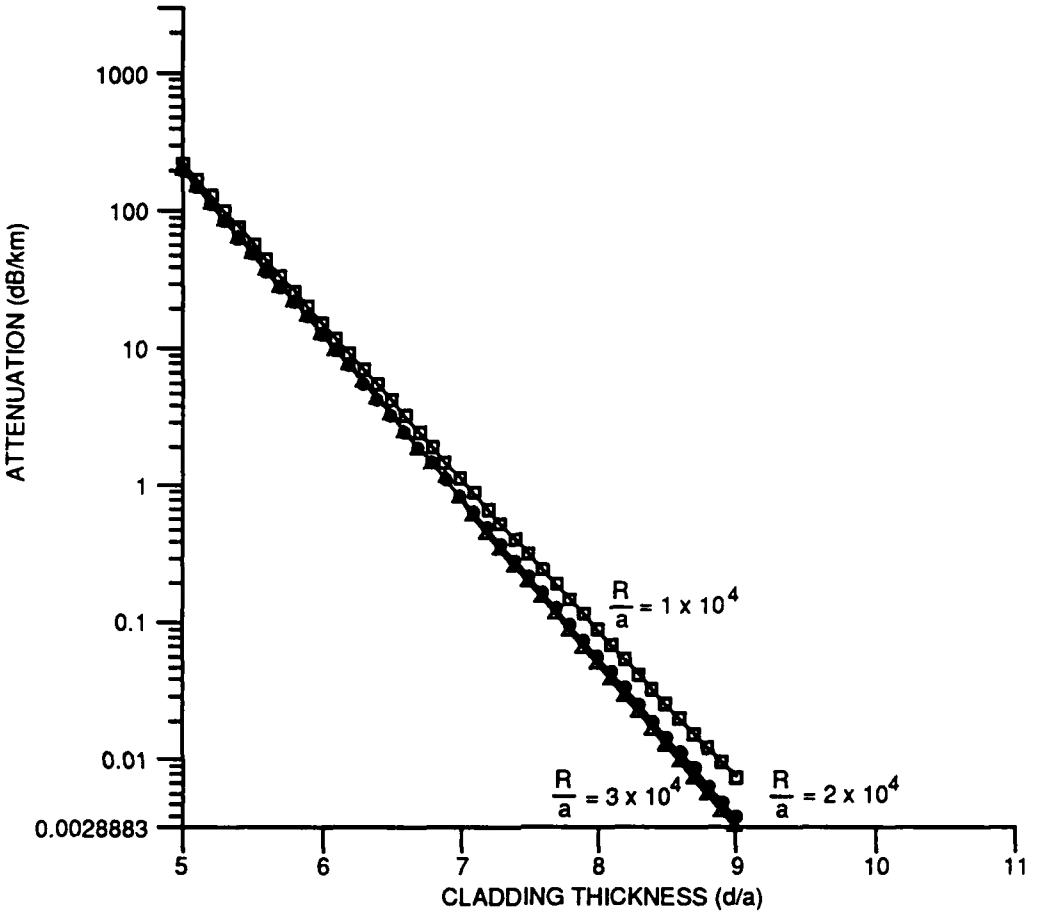

wavelength (μm) = 1.30	n1 = 1.4600
core radius (μm) = 2.50	n2 = 1.4497
Δ_1= .7%	n3 = 1.4600

FIGURE 9. Normalized Cladding Thickness Versus Attenuation for AT&T TVF at 1.3 μm.

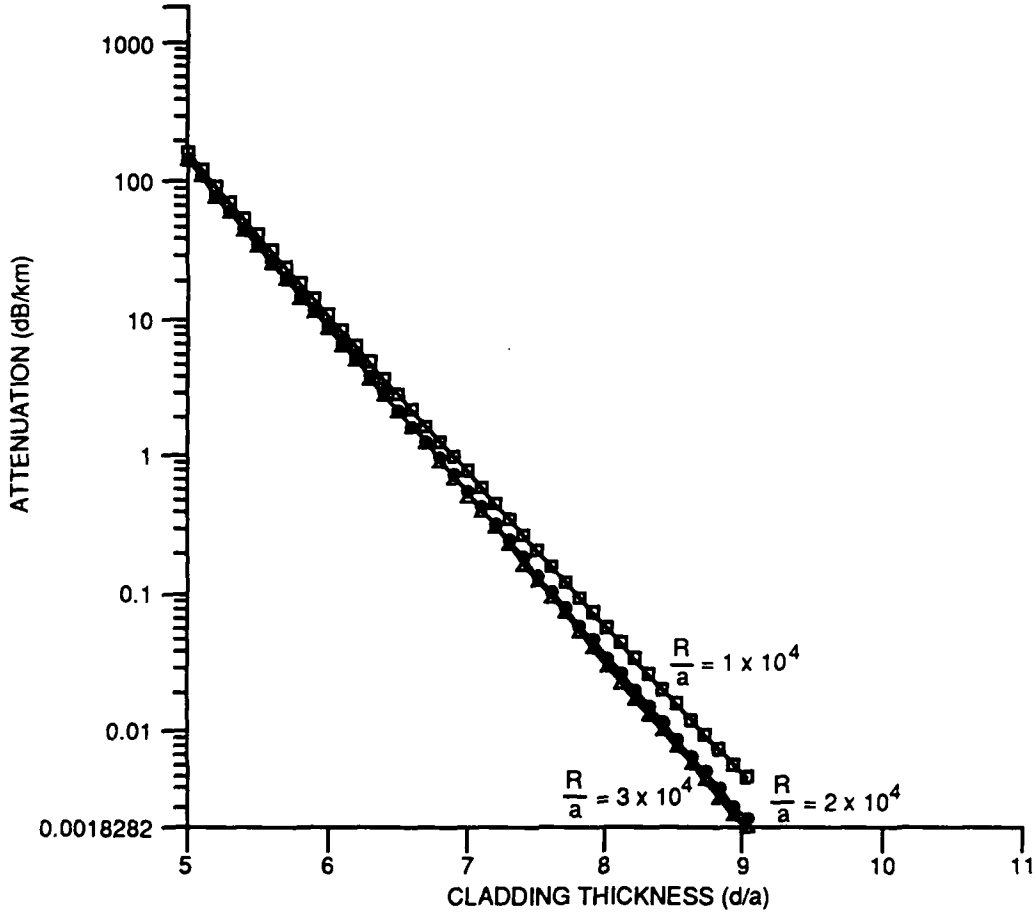

wavelength (μm) = 1.55	n1 = 1.4600
core radius (μm) = 3.00	n2 = 1.4497
Δ_1 = .7%	n3 = 1.4600

FIGURE 10. Normalized Cladding Thickness Versus Attenuation for AT&T TVF at 1.55 μm.

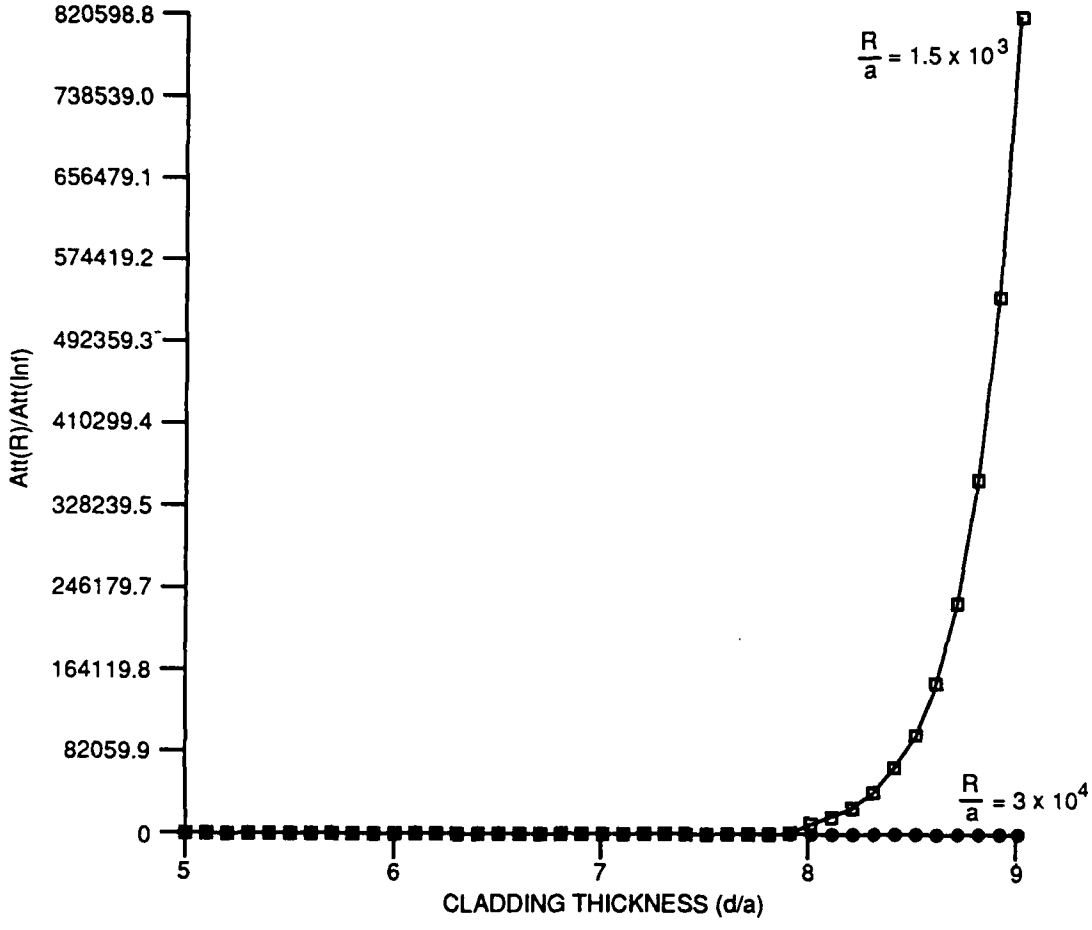

wavelength (μm) = 1.30	n1 = 1.4640
core radius (μm) = 2.75	n2 = 1.4497
Δ_1= .98%	n3 = 1.4640

FIGURE 11. Normalized Cladding Thickness Versus Normalized Attenuation for Corning Payout Fiber at 1.3 μm.

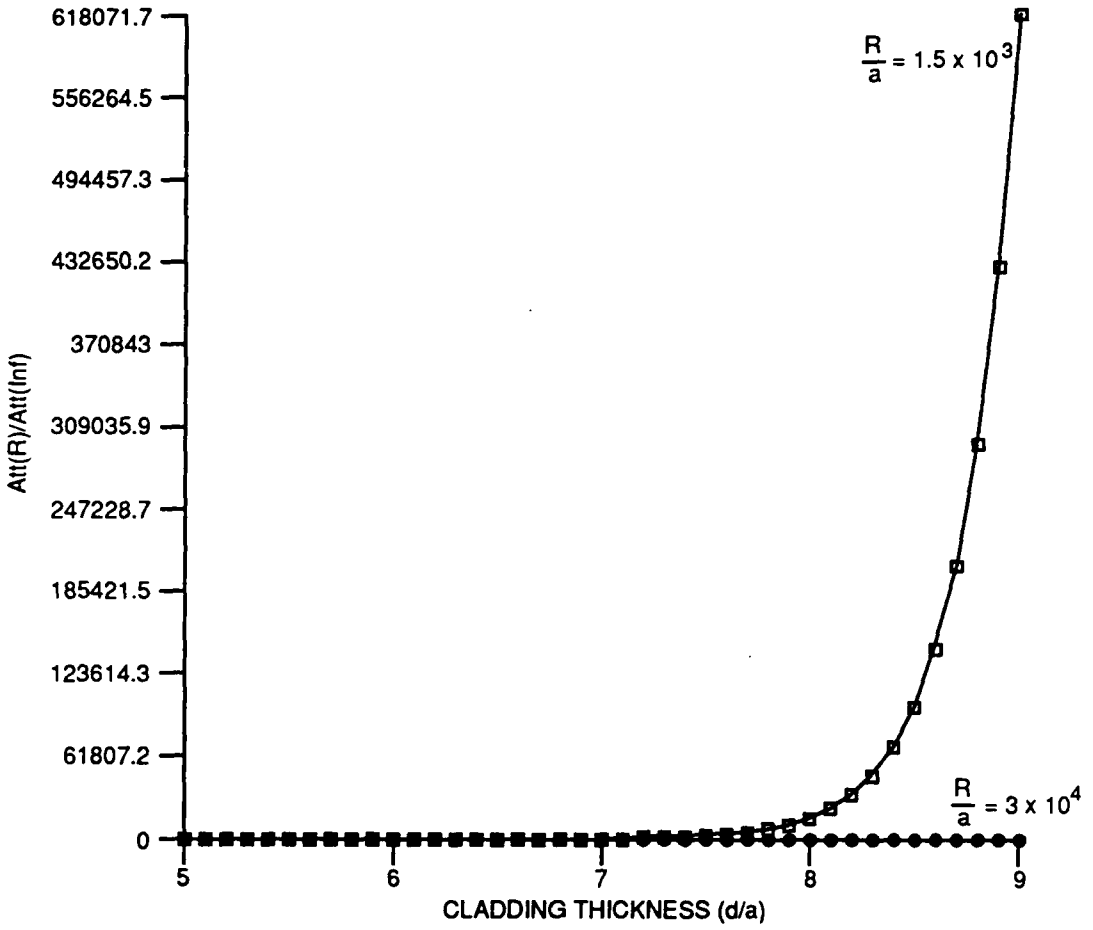

wavelength (μm) = 1.55	n1 = 1.4640
core radius (μm) = 3.00	n2 = 1.4497
Δ_1= .98%	n3 = 1.4640

FIGURE 12. Normalized Cladding Thickness Versus Normalized Attenuation for Corning Payout Fiber at 1.55 μm.

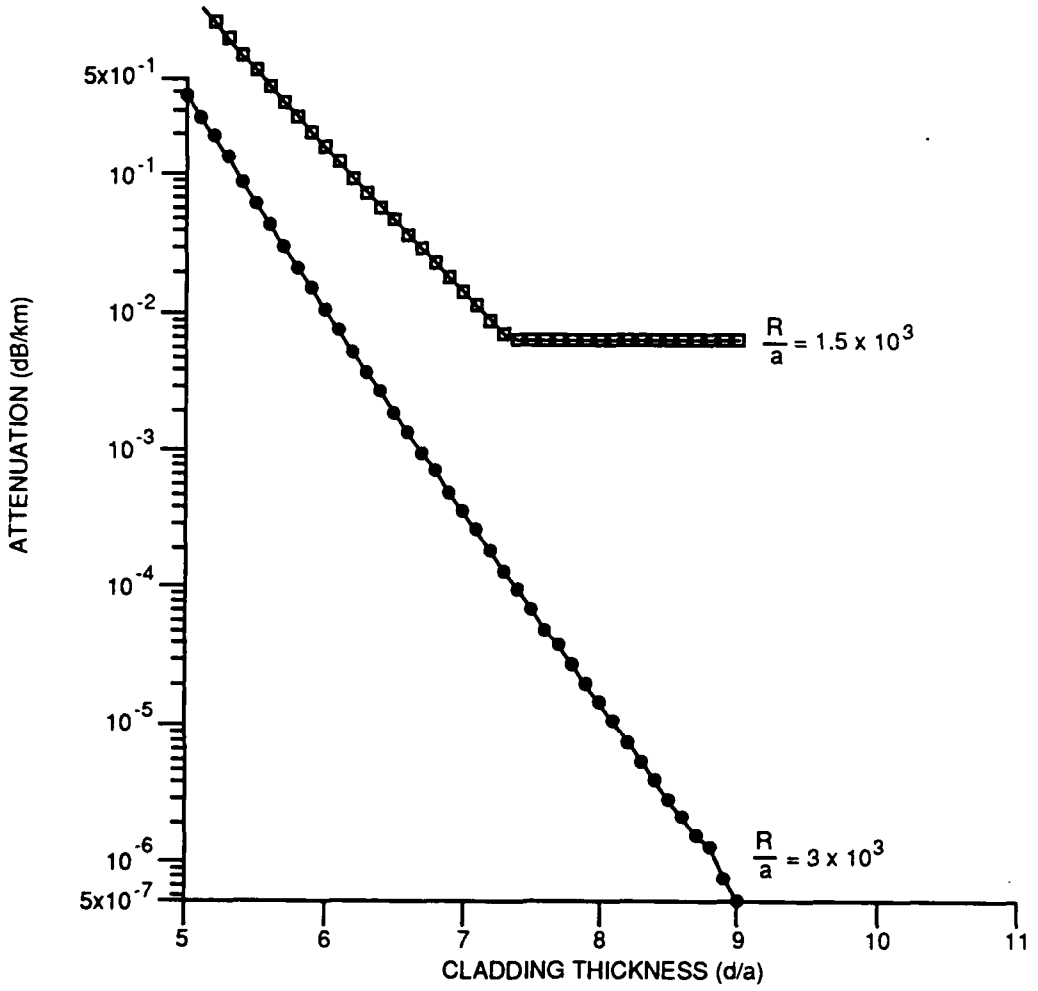

wavelength (μm) = 1.30	n1 = 1.4640
core radius (μm) = 2.75	n2 = 1.4497
Δ_1= .98%	n3 = 1.4640

FIGURE 13. Normalized Cladding Thickness Versus Attenuation for Corning Payout Fiber at 1.3 μm.

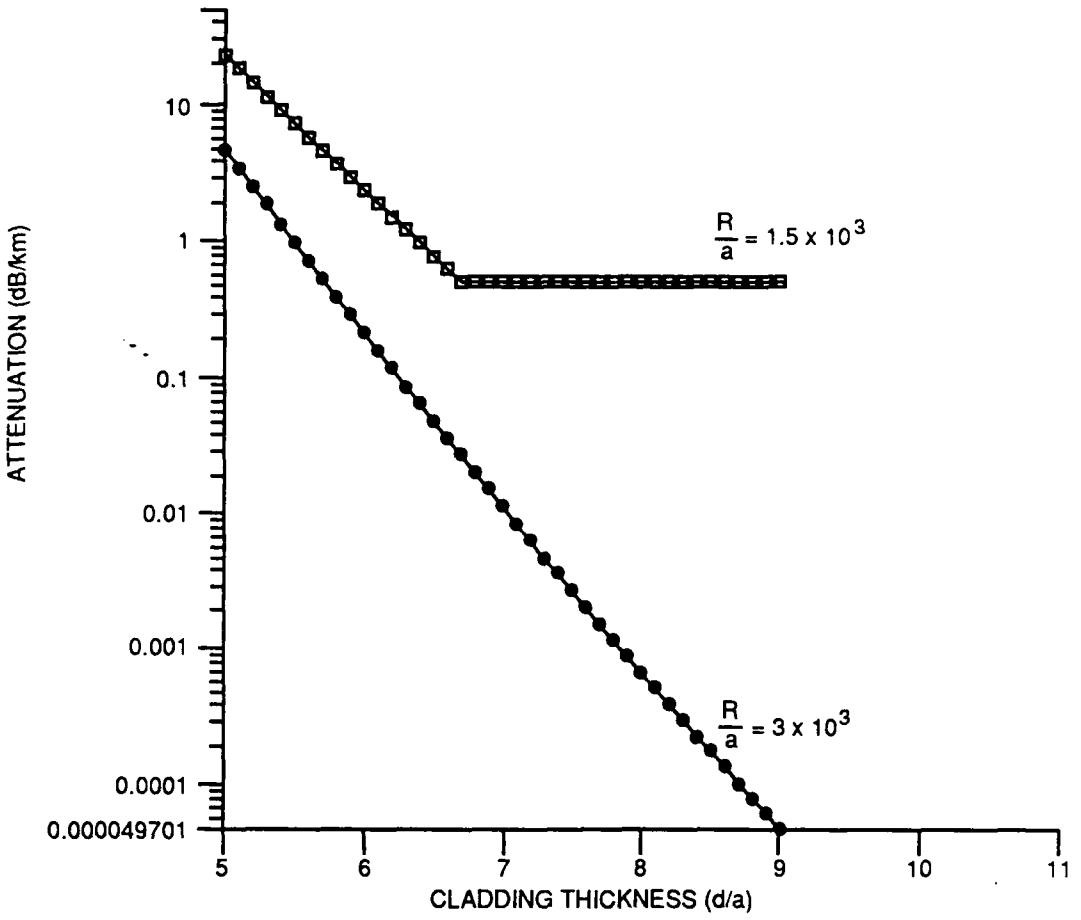

wavelength (μm) = 1.55	n1 = 1.4640
core radius (μm) = 3.00	n2 = 1.4497
Δ_1= .98%	n3 = 1.4640

FIGURE 14. Normalized Cladding Thickness Versus Attenuation for Corning Payout Fiber at 1.55 μm.

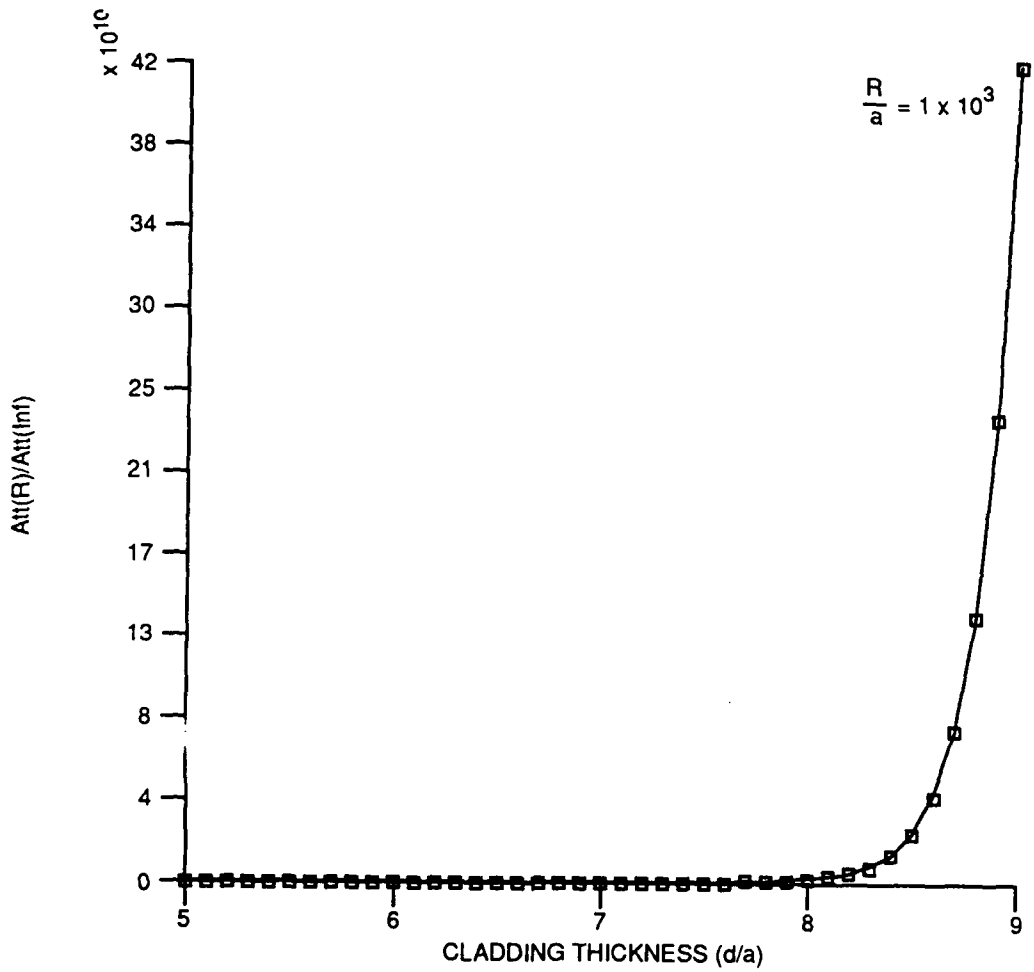

wavelength (μm) = 1.55	n1 = 1.4640
core radius (μm) = 4.05	n2 = 1.4497
Δ_1= .98%	n3 = 1.4640

FIGURE 15. Normalized Cladding Thickness Versus Normalized Attenuation for Corning SMF/DS at 1.55 μm.

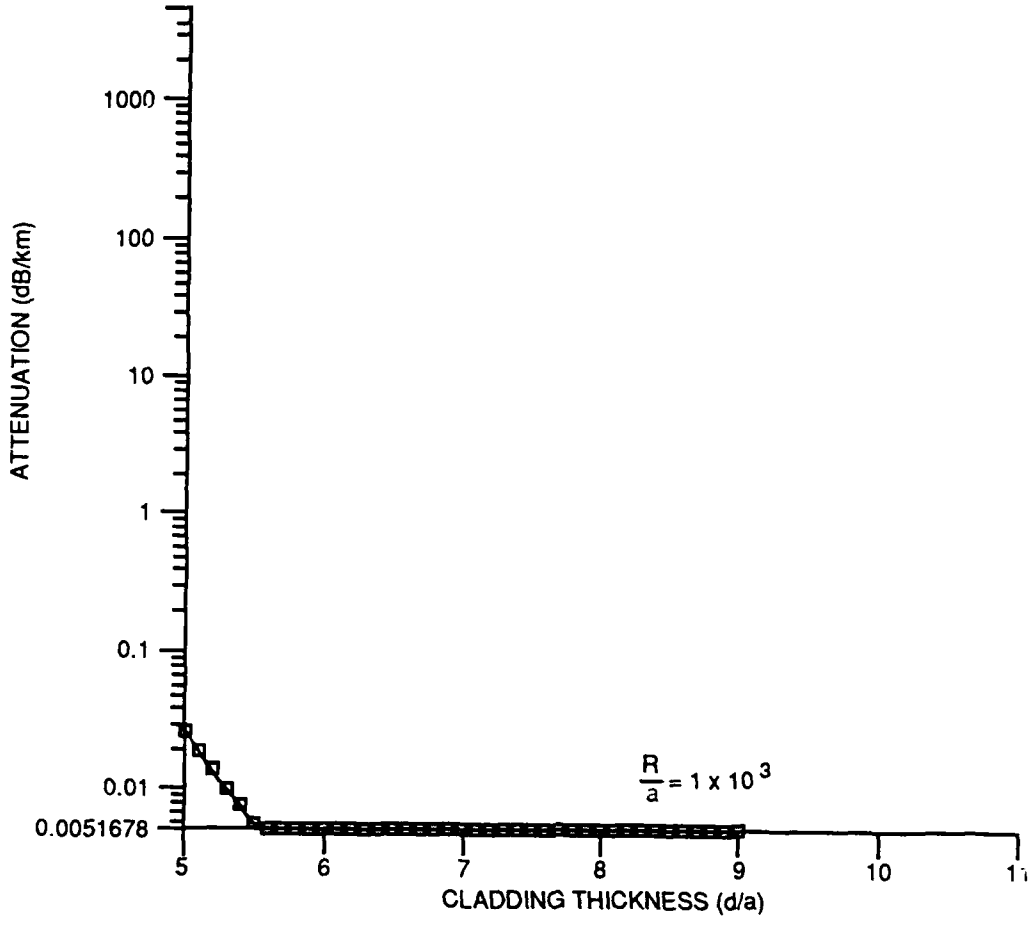

wavelength (μm) = 1.55	n1 = 1.4640
core radius (μm) = 4.05	n2 = 1.4497
Δ_1= .98%	n3 = 1.4640

FIGURE 16. Normalized Cladding Thickness Versus Attenuation for Corning SMF/DS at 1.55 μm.

INITIAL DISTRIBUTION

2 Naval Air Systems Command (AIR-5004)
2 Naval Sea Systems Command (Technical Library)
1 Commander in Chief, U. S. Pacific Fleet, Pearl Harbor (Code 325)
1 Commander, Third Fleet, San Francisco
1 Commander, Seventh Fleet, San Francisco
2 Naval Academy, Annapolis (Director of Research)
1 Naval War College, Newport
1 Air Force Intelligence Agency, Bolling Air Force Base (AFIA/INTAW, MAJ R. Esaw)
2 Defense Technical Information Center, Alexandria
1 Gonzaga University, Spokane, WA (Physics Department, Prof. S. Hoffmaster)
1 Hudson Institute, Incorporated, Center for Naval Analyses, Alexandria, VA (Technical Library)